

# Batch Adsorption of Ammonium Ions from Synthetic Wastewater using Local Cameroonian Clay and ZnCl<sub>2</sub> Activated Carbon

Zing Zing Bertrand, Belibi Belibi Placide Désiré, Ankoro Naphtali Odogu, Kouotou Daouda, Ndi Julius Nsami, Ketcha Joseph Mbadcam

**Abstract**— Local Cameroonian clay and ZnCl<sub>2</sub> activated carbon were used for the adsorption of NH<sub>4</sub><sup>+</sup> ions from synthetic wastewater. The Batch adsorption experiments were conducted and optimal conditions were established to better understand the effects of solution pH, initial ammonium ions concentration, adsorbents dose and contact time. The time-dependent experimental studies showed that, the adsorption quantity of ammonium ions increases with initial concentration and decrease with adsorbents dose. The ammonium ions uptake was very fast and reached equilibrium within 10 and 15 min with ZnCl<sub>2</sub> activated carbon and Soukamna Clay. Both ZnCl<sub>2</sub> activated carbon and Soukamna Clay gave best adsorption results at pH 2 and 6. FTIR, powder X-ray diffraction, chemical analysis, TGA and DSC analysis were used to characterize the Soukamna Clay. The adsorption equilibrium were confronted using Langmuir, Freundlich, Temkin and D–K–R isotherm models and their applicability were judged by comparing the correlation coefficients and the experimental calculated quantities. The D–K–R, Temkin and Freundlich isotherms models best fitted to the experimental data for Soukamna Clay while the D–K–R isotherm model fitted well with ZnCl<sub>2</sub>-AC. The adsorption mechanism was analyzed using the pseudo-first order, pseudo-second order, the Elovich kinetic and intra-particle diffusion models. The pseudo-second order kinetic model correlates better the experimental and calculated data than the other three kinetic models which suggests that, chemisorption was more dominant with both adsorbents. Soukamna Clay and ZnCl<sub>2</sub>-AC used successfully as a low-cost adsorbent for the removal of NH<sub>4</sub><sup>+</sup> ions from aqueous solution can have promising application in industrial wastewater treatment.

**Index Terms**— Activated carbon, Ammonium Ions, Batch Adsorption, Soukamna Clay.

## I. INTRODUCTION

The nitrogenized nutrition is one of the essential constituent to enhance agricultural productivity [1]. In order not to mortgage the yield, farmers seek on how to enrich the soil with nitrogen. To match up with the task, they use many methods of remedy like rotation, organic contributions, fertilizers etc. But, only 25 to 30% of ammonium in these fertilizers is assimilated by plants; 70% is run out to be accumulated in water [2]. Despite the fact that nitrogen pollution can be obtained from fertilizers, it can also be from municipal sewage, industrial wastewater and agricultural

wastes decomposed from organic nitrogen like animal dejection [3]. Thus, it is essential to control the ammonium content in water.

The European Union limited the content of ammonium ions in consumption water to be less than 0.50 mg/L [4]. High percentages of these ions in water constitute an awkward element because they interfere with chloride ions to form chloramines which modify the odor and the taste of water [5]. The inhalation of ammonium ions causes cough and redness when it comes in contact with the skin or the eye. Its ingestion causes nausea of the throat, vomiting and diarrhea [6]. In extreme cases, water rich in ammonium ions corrode soils building materials [7], decreases oxygen required for the breathing of the watery species, causes massive development of algae which leads to the eutrophication and finally to the toxicity of aquatic organisms [8]. Therefore, it is necessary to eliminate them from water.

Many depollution methods of ammonium ions have been developed such as biological nitrification and denitrification, air stripping, chemical precipitation, electrocoagulation, reverse osmosis, ions exchange, breakpoint chlorination and adsorption [9-13]. These methods of elimination are effective and expensive that limits their application. Hence, finding less costly methods of elimination is important to combat this pollutant. Adsorption is a simple separation method which is an adhesion of liquid or gas to solid surface by creation of a thin layer of the adsorbate on the adsorbent surface [14]. This method uses natural and available materials at low cost, easy to employ and regenerated [15]. Many adsorbents have been used to eliminate ammonium ions such as alumina, zeolite, iron oxide and activated carbon [16-18]. Much work has been done using commercial activated carbons and clays in the adsorption of heavy metals and dyes [19-21]; but ammonium sorption in synthetic wastewater has not yet been investigated sufficiently.

In the present study, attempts have been made to develop low cost adsorbents using ZnCl<sub>2</sub> activated carbon (ZnCl<sub>2</sub>-AC) and Soukamna Clay (SC) for the adsorption of ammonium ions from synthetic wastewater due to their natural abundance, nontoxicity and porous structures. The valorization of these local materials was to minimize the problem of high cost involved in the treatment of industrial wastewaters in Cameroon and most developing nations. The effect of initial ammonium ions concentration, pH, adsorbents dose and contact time were investigated. Equilibrium and kinetic parameters were also determined to help provide better understanding of the adsorption process.

Zing Zing Bertrand, Belibi Belibi Placide Désiré, Ankoro Naphtali Odogu, Kouotou Daouda, \*Ndi Julius Nsami, Ketcha Joseph Mbadcam, Physical Chemistry Laboratory, Department of Inorganic Chemistry, Faculty of Science, University of Yaoundé I, B.P. 812, Yaoundé – Cameroon, \*Corresponding author

## II. EXPERIMENTAL METHODS

### 1.1. Preparation of clay material

In the present work, clay mineral was collected at a depth of 150 cm from a deposit locality of Soukamna village, 6 km from Mayo Danay division in the Far North region of Cameroon. After collecting the raw clay lumps, stones and other heavy particles were removed from the samples by sieving. The clay material was then crushed and 1 kg of the obtained powder was dispersed in 10 L of permuted water to prepare a milky clay suspension. After sedimentation of the clay particles, the top part of the supernatant was recovered and filtered through a 50 mm sieve to remove the larger non-clay fractions and to obtain the fine clay fraction. The suspensions were then dried at 110°C in an oven until complete evaporation of water. It was then crushed in a porcelain mortar and sieved with a sieve (Bs410-1: 2000, Aperture: 50 MIC, N° 0062488) of mesh diameter 50 µm. The powder obtained was dried at 110° C in oven for 24 hours to eliminate water of crystallization and stored in a desiccator containing CaCl<sub>2</sub> (drying agent) ready for used.

### 1.2. Cola Nut Shells

The Cola Nut shells were collected from the North-West region of Cameroon precisely in the Donga-Mantung division. The preparation of activated carbon was done according to Ndi *et al.* (2014) [22].

### 1.3. Characterization Techniques

The chemical composition of clay was analyzed using a wavelength dispersive X-ray fluorescence apparatus (Shimadzu, XRF-1800) to evaluate the proportions of impurities in the raw material as well as the loss on ignition (LOI). In addition, powder X-ray diffraction crystallography (DRX) analysis was performed to put in evidence; the mineralogical composition of clay using a Philips X'Pert PRO diffractometer equipped with Ni-filtered Cu-Kα (λ = 1.542 Å) radiation. The apparatus operated at 40 kV and 100 mA in a step scan mode. Diffraction patterns were collected at a scanning speed of 0.0167° s<sup>-1</sup>. Thermo-gravimetric analysis (TGA) and Differential scanning calorimetry (DSC) analysis were performed using a 2960 TA instrument under argon from room temperature up to 1200°C at a heating rate of 5°C/min. The Fourier Transformation Infrared Spectroscopy (FTIR) of both adsorbents was acquired on a Bruker alpha-p spectrometer using KBr pellet method at room temperature to identify the functional groups present on the adsorbents surface. The physico-chemical properties of Soukamna Clay and ZnCl<sub>2</sub> activated carbon are listed in *Table 1*.

### 1.4. Chemical Reagents

Analytical grade reagents were supplied in powdered form by Merck and were used without further purification for the preparation of synthetic aqueous solution.

### 1.5. Preparation of Solutions

#### 1.5.1. Ammonium Ions Solution

All the experiments were conducted with synthetic wastewater. A stock solution of ammonium ions of concentration 5000 mg/L was prepared by dissolving (7.4580 ± 0.0001) g of ammonium chloride salt in a 500 mL volumetric flask, agitated by using a magnetic stirrer for a period of time and complete with distilled water up the mark.

This solution was again stirred with a magnetic stirrer for two hours to obtain homogeneity. Standard solutions of various concentrations were obtained by dilution. Solution of hydrochloric acid (0.1 M) and sodium hydroxide (0.1 M) were also prepared for pH adjustments.

## III. BATCH ADSORPTION EXPERIMENTS

The batch adsorption experiments studies were conducted at room temperature (25°C) in 250 mL screw-capped conical flask. For each run, 0.05 – 0.5 g of the adsorbent dosage were weighed and placed in the flask containing 20 mL solution of ammonium ions of desired concentration (from 2000 to 4500 mg/L). The pH values were varied between 2 and 8. The suspension was stirred for an interval of time between 5 – 35 min using magnetic stirrer at a controllable speed. After agitation, the suspensions were filtered using Whatman filter paper N° 1. The concentrations of the filtrate were determined by back titration method using methyl red as indicator [23]. The quantity adsorbed by a unit mass of an adsorbent at equilibrium (Q<sub>e</sub>) and the percentage adsorbed (% R) in an instant were calculated using relations (1) and (2) respectively,

$$Q_e = \frac{(C_o - C_t)}{m} V \quad (1)$$

$$\%R = \frac{(C_o - C_t)}{C_o} \times 100\% \quad (2)$$

Where C<sub>e</sub> and C<sub>t</sub> are respectively the concentration of adsorbate at equilibrium and at time t; C<sub>o</sub> is the initial concentration; m is the mass of the adsorbent and V is the volume of the adsorbate.

## IV. RESULTS AND DISCUSSION

### 4.1. Adsorbent Characterization

#### 4.1.1. Chemical analysis of Soukamna clay

The chemical analysis of Soukamna clay shown in *Table 2* constitute mainly of: SiO<sub>2</sub>, Al<sub>2</sub>O<sub>3</sub>, Fe<sub>2</sub>O<sub>3</sub>, CaO, K<sub>2</sub>O and TiO<sub>2</sub>. The other oxides are in traces. Moreover, the ratio  $\frac{\% \text{SiO}_2}{\% \text{Al}_2\text{O}_3} = 3.42$  ranging between 2.5 and 5 shows that, the Soukamna clay is of type Smectite and precisely Montmorillonite [24].

#### 4.1.2. Powder X-ray Diffraction of Soukamna Clay

The powder X-Ray diffraction crystallography of Soukamna Clay represented in *Figure 2* shows the existence of quartz, anorthite and kaolinite in crystalline phases.

#### 4.1.3. Fourier Transform Infrared Spectroscopy (FTIR) of Soukamna Clay

The FTIR Analysis results depict the absorbance spectra of Soukamna Clay. *Figure 3* shows the pick at 3692 cm<sup>-1</sup> which corresponds to -OH group of the interstitial water, the vibration bands at 3621 cm<sup>-1</sup> and deformation at 910 cm<sup>-1</sup> and 793 cm<sup>-1</sup> can be attributed to the presence of Al-OH due to coordination between dependent water and an aluminum atom of the octahedral layer and this indicate that, the clay is dioctahedral [25]. The vibration band located around 1626 cm<sup>-1</sup> and 1434 cm<sup>-1</sup> corresponds to the deformation vibrations

of H-O-H due to the molecules of adsorbed water between the layers. The vibration bands observed at 1025 and 443  $\text{cm}^{-1}$  could be allotted to the deformation vibrations of Si-O-H [26]. According to Subbareddy (2014) [27], the stretching vibration of the Si-O usually appears in montmorillonites at 1100  $\text{cm}^{-1}$ . Here, this band is located at 997  $\text{cm}^{-1}$ ; this light displacement towards the lower frequency would be due to the substitution of silicon in tetrahedral sites by the trivalent ions ( $\text{Al}^{3+}$ ) and also to the substitution of the  $\text{Al}^{3+}$  ions in octahedral sites by the  $\text{Fe}^{3+}$  ions. The appearance of the deformation bands around 528  $\text{cm}^{-1}$  shows the Si-O-Al vibrations and 458  $\text{cm}^{-1}$  for the Si-O-Mg vibrations and around 414  $\text{cm}^{-1}$  for the Si-O-Si vibrations [28]. The band located at 681  $\text{cm}^{-1}$  could correspond to the deformation vibration of quartz. The interpretation of this spectra shows that, the adsorption of ammonium ions by Soukamna clay is done without modification of the material structure and thus leads to physisorption.

#### 4.1.4. Fourier Transform Infrared Spectroscopy (FTIR) $\text{ZnCl}_2$ activated carbon

The FTIR Analysis results depict the absorbance spectra of  $\text{ZnCl}_2$  Activated Carbon. From *Figure 4*, the pick at 3368  $\text{cm}^{-1}$  corresponds to -OH of aliphatic alcohols. The band at 3267  $\text{cm}^{-1}$  corresponds to the elongation vibrations -OH of phenol group [29]. The band observed at 3105  $\text{cm}^{-1}$  is due to the valence vibration -NH of the primary amine. The band observed at 1567  $\text{cm}^{-1}$  is attributed to -C=C- bond aromatic rings and 870  $\text{cm}^{-1}$  to 819  $\text{cm}^{-1}$  for the Meta and di substituted benzene. The band located at 1166  $\text{cm}^{-1}$  is that of the valence vibration C-O of alcohols group. The bands observed around 1060  $\text{cm}^{-1}$  and 1031  $\text{cm}^{-1}$  correspond to the valence vibration of C-C while the bands around 793  $\text{cm}^{-1}$  to 746  $\text{cm}^{-1}$  are that C-Cl. The bands located from 1250 to 1000  $\text{cm}^{-1}$  are those of deformation vibration of the C-N of primary amines. Those located around 931  $\text{cm}^{-1}$  to 660  $\text{cm}^{-1}$  could correspond to the deformation vibrations of the aromatic rings para and Meta substituted. The bands located at 2939  $\text{cm}^{-1}$  and 2843  $\text{cm}^{-1}$  could respectively be due to the symmetrical elongation vibrations of -  $\text{CH}_3$  / -  $\text{CH}_2$  of alkanes while those appearing around 1329  $\text{cm}^{-1}$  and 1280  $\text{cm}^{-1}$  could correspond to the deformation vibrations of - CH of alkanes. The bands located at 1098  $\text{cm}^{-1}$  and 1025  $\text{cm}^{-1}$  could correspond to those of C-O group; those located from 627  $\text{cm}^{-1}$  to 587  $\text{cm}^{-1}$  could be due to the presence of the functions C-Cl and  $\text{CCl}_3$  into activated carbon. Finally the bands observed at 547  $\text{cm}^{-1}$  and 517  $\text{cm}^{-1}$  could correspond to the deformation vibrations of O-Zn[22]. This interpretation proves that, the ammonium sorption onto  $\text{ZnCl}_2$ - AC is done with modification of the material structure and thus leads to a chemisorption process.

#### 4.2. Effect of contact time

The agitation time which is one of the most important factors affecting the adsorption efficiency was evaluated. The quantity adsorbed with respect to agitation time was plotted and shown in *Figure 5*. According to the graph, the quantity of ammonium ions adsorbed increase rapidly within the first ten minutes and reaches equilibrium at 15 minutes with Soukamna Clay (SC) and rapidly within the first five minutes with  $\text{ZnCl}_2$  activated carbon ( $\text{ZnCl}_2$  - AC) and reaches equilibrium at 10 minutes where no further adsorption took place. The increase rate of adsorption at the beginning could be due to the availability of adsorption sites. Thereafter,

saturation leading to equilibrium. These results are similar to those obtained by Fumba *et al.* (2014)[30].

#### 4.3. Effect of adsorbents dose

Adsorption experiments were performed at different adsorbents doses (0.1, 0.2, 0.3, 0.4, and 0.5 g) of SC and  $\text{ZnCl}_2$  - AC. *Figure 6* shows that, the quantity adsorbed decreases with an increase in adsorbent dose. The reduction of quantity adsorbed with the increase in mass of the adsorbents is due to agglomeration of the particles which form aggregates and obstruct the pores and thus prevent intra-particle diffusion into the pores of  $\text{ZnCl}_2$ -AC[31]. While with Soukamna Clay, this agglomeration reduces the electrostatic force between the layers and disguises the adsorption sites [32]. In addition, the decrease in adsorption capacity may be also due to the overlapping of the adsorption sites as a result of overcrowding of adsorbent particles.

#### 4.4. Effect of pH

The pH greatly influences the ammonium sorption. *Figure 7* shows that, the adsorption of ammonium ions by  $\text{ZnCl}_2$ -AC is maximum at pH = 2 ( $Q_e = 152.43 \text{ mg/g}$ ). This may be due to the formation of hydrogen bond between heteroatoms of  $\text{ZnCl}_2$  - AC surface and the hydrogen of the ammonium ions[33]. It is noted that, at pH  $\geq 6$  for this same adsorbent the amount of hydroxides ions becomes significant in the medium. Thus, strong attraction between the  $\text{NH}_4^+$  ions and the carboxylate groups (resulting from deprotonation of carboxylic acid function by the hydroxides ions) of  $\text{ZnCl}_2$ -AC are created. According to some authors, at pH  $\geq 6$ , the silanols groups of clays are in the anionic forms and induce negative charge on the surface of Soukamna Clay. These negatives sites enhance the binding of  $\text{NH}_4^+$  ions onto SC [16, 34] and attained the adsorbed quantities of 338.14 mg/g.

#### 4.5. Effect of initial ammonium concentration

*Figure 8* shows that, the increase in the initial concentration of  $\text{NH}_4^+$  ions brings an appreciable increase in the quantities adsorbed for both adsorbents. This is due to the increase in collision forces between  $\text{NH}_4^+$  ions in solution which break the resistance forces on the surface of both adsorbents. Thus, facilitate the diffusion of  $\text{NH}_4^+$  ions into the pores. The retention curve of  $\text{NH}_4^+$  ions by  $\text{ZnCl}_2$ -AC, has a parallel stage with the concentrations axis (3500 and 4000 mg/g). This is due to the total occupation of micropores (saturation) with formation of monolayer coverage. It is also observed that, at 4500 mg/g the quantity adsorbed increases with the formation of a second layer with weak energy which characterizes physisorption [35].

#### 4.6. Adsorption isotherms models

The adsorption isotherms of  $\text{NH}_4^+$  ions on both adsorbents are plotted with  $Q_e$  against  $C_e$  as shown in *Figure 7*. It describes the retention of ammonium from aqueous medium to solid phase at constant temperature and pH. The adsorption equilibrium is established when the adsorbent surface is brought into contact with adsorbate phase for sufficient time. The adsorption modeling isotherms shows that, the ammonium sorption on both adsorbents obeys isotherm of type IV which is characterized by strong interactions on the monolayer coverage and weak interaction on the multilayer coverage of the adsorbate on the surface of the adsorbent [30]. The Data obtained from these studies were then fitted using

four isotherms such as Langmuir, Freundlich, Dubinin-Kaganer-Radushkevich (D-K-R) and Temkin models (Table 3). The graphs of all isotherms models are shown in Figure 10, 11, 12 and 13.

The applicability of these isotherm equations to adsorption process was judged based on the correlation coefficients ( $R^2$ ) and the comparison between the calculated and experimental values of quantities adsorbed at equilibrium. The correlation coefficients and the values of intercept are given in Table 4. These results show that, the isotherms models of linear correlation coefficient with close unit include D-K-R, Temkin, Freundlich and Langmuir for SC whereas, with ZnCl<sub>2</sub>-AC only the isotherms of Langmuir and D-K-R are near to the unit. The good correlation of the experimental data with the Langmuir isotherm indicates a specific adsorption for both adsorbents [31]. It is also observed that, the intensity of adsorption  $K_L$  of ZnCl<sub>2</sub>-AC is higher than that of SC, thus translate a good affinity between ammonium ions and ZnCl<sub>2</sub>-AC [36]. Although it agrees with the interpretation of the infrared spectra of ZnCl<sub>2</sub>-AC, it disagrees with that of SC. Furthermore, the gap between the calculated and experimental values of adsorbed quantities is larger. Therefore, we can conclude here that, this model does not describe well the ammonium sorption with both adsorbents. The Freundlich isotherm, described the isotherm data with high-correlation coefficients for SC, a low one was observed for ZnCl<sub>2</sub>-AC. But the adsorption capacity  $K_F$  which indicates the strength of the relationship between adsorbate and adsorbent of ZnCl<sub>2</sub>-AC is 5.40 times larger than SC; can be due to the heterogeneous surface of ZnCl<sub>2</sub>-AC with a prevalence of acid functions [22]. Moreover,  $1/n$  of ZnCl<sub>2</sub>-AC compared to SC shows that, ZnCl<sub>2</sub>-AC is more heterogeneous than SC [38]. The ammonium sorption with both adsorbents is initially done into monolayer coverage then into multilayer coverage with characteristic of physical adsorption. Furthermore, the higher regression value of SC ( $R^2 = 0.9837$ ) compared to that of ZnCl<sub>2</sub>-AC ( $R^2 = 0.8786$ ) also shows that, the Temkin isotherm confirms typical adsorption due to weak interactions adsorbate-adsorbent characteristic of physisorption [34].

The Dubinin-Kaganer-Radushkevich isotherm gives a better linear correlation coefficient with Soukamna Clay ( $R^2 = 0.9865$ ) in relation to ZnCl<sub>2</sub>-AC ( $R^2 = 0.9494$ ). The mean sorption energies obtained are lower than 8 kJ/mol for both adsorbents indicates a physical adsorption [38]. Moreover, the calculated and experimental quantities being close, hence describes well the adsorption process. The interpretation of these three last isotherms fit well with the infrared spectra of SC and the isotherm of type IV confirming a physical adsorption.

### 4.7. Adsorption kinetic models

Adsorption kinetic models are areas of analytical chemistry relating to the rate and speed at which the chemical reaction occurs. In surface and interface chemistry, kinetic models are used to evaluate the adsorption mechanism of adsorbate on the surface of adsorbent. The four kinetic models used are consigned in Table 5. The fitting parameters of the four kinetic models and the correlation coefficients are given in Table 6. Poor correlation coefficients of kinetic data with the pseudo-first order, intra-particle diffusion and Elovich models were observed. But, well described by the

pseudo-second order; the high value of constant  $K_2$  for ZnCl<sub>2</sub>-AC compared to SC suggested that, ammonium could be rapidly sequestered by carbon functional groups, resulting in the system quickly reaching equilibrium [39]. The confirmation of pseudo-second order kinetic also indicates that, chemisorption is the rate-limiting step in adsorption process [17]. This result corroborates with the infrared spectra of the ZnCl<sub>2</sub>-AC which predicted chemisorption. Furthermore, the calculated and the experimental quantities values are closed and further confirm the pseudo-second order kinetic model [27]. The intra-particle diffusion involves in the adsorption process if the line passes through origin; then intra-particle diffusion is the rate limiting step. The lines do not pass through the origin suggesting that, pore diffusion is the only controlling step and not the film diffusion [40]. Moreover, even if Elovich kinetic model does not predict any definite mechanism, but it is usefully found to describe chemical adsorption on highly heterogeneous adsorbents [41].

## V. CONCLUSION

The present investigation shows that, ZnCl<sub>2</sub>-AC and SC can be used effectively as efficient adsorbents for the removal of NH<sub>4</sub><sup>+</sup> ions from synthetic wastewater. The amount of NH<sub>4</sub><sup>+</sup> ions adsorbed highly depend on contact time, initial NH<sub>4</sub><sup>+</sup> concentration, solution pH and adsorbents dosage. The removal of ammonium ions is optimum in acidic pH for both adsorbents. The adsorption of NH<sub>4</sub><sup>+</sup> ions on both adsorbents followed pseudo-second order kinetic model while the isotherms studies describe physical adsorption.

## ACKNOWLEDGEMENT

The authors sincerely thank the Unit 'Adsorption and Surface' of the Applied Physical and Analytical Chemistry Laboratory of the University of Yaoundé I. They are also grateful to the scholars whose articles are cited and included in references of this manuscript and grateful to authors, editors, and publishers of all the articles, journals and books from where the literature for this article has been reviewed and discussed.

## REFERENCES

- [1] P. Buragohain, Dr S. Sredeep and Dr S. Nadia, "A Study on the Adsorption of Ammonium in Bentonite and Kaolinite", *International Journal of Chemical, Environmental and Biological Sciences*, Vol. 1, No. 1, 2013, pp. 1-4.
- [2] S. Jolly, J. Mullot and J. Emery, "Mise au Point de Méthodes d'Analyse en Flux Séquentiel: Nitrite, Nitrate et Ammonium Application pour la Détermination de l'Acceptabilité Réglementaire d'Eaux Destinées à la Consommation Humaine et pour la Surveillance de l'Environnement: Rapport de Stage de Master France", *LASEM*, 2010, p. 62.
- [3] O. I. El-Shafey, N. A. Fathy and T. A. El-Nabarawy, "Sorption of Ammonium Ions onto Natural and Modified Egyptian Kaolinites: Kinetic and Equilibrium Studies", *Advanced in Physical Chemistry*, Vol. 2014, 2014, pp. 1-12.
- [4] A. Negrea, L. Lupa, C. Muntean, M. Ciopec, C. Ghimboasă and M. Motoc, "Studies Regarding the Possibilities of Ammonium Ions Removal from Underground Waters", *Series of Chemistry and Environmental Engineering*, Vol. 53, 2008, pp. 1-2.
- [5] H. Bedelea, A. Măicăneanu, S. Burcă, and M. Stanca, "Romanian Zeolitic Volcanic Tuffs and Bentonites Used to Remove Ammonium

- Ions From Wastewaters”, *Hellenic Journal of Geosciences*, Vol. 45, 2012, pp. 23-32.
- [6] T. Nadejda, “Removal of Ammonium and Phosphate from Aqueous Solutions by Activated and Modified Bulgarian Clinoptilolite”, *Journal of Chemical Engineering and Materials Science*, Vol. 3, 2012, pp. 79-85.
- [7] L. Youcef, A. Ouakou, D. Boulanouar and S. Achour, “Étude du Pouvoir Adsorbant du Charbon Actif en Poudre pour l’Élimination des Phosphates des Eaux Naturelles”, *Larhyss Journal*, 17, 2014, pp. 35-46.
- [8] H. Wissem and S. Mongi, “Ammonium Sorption by Soils Profile of Semi-Arid Areas”, *Journal of Environmental Science, Toxicology and Food Technology*, Vol. 9, No. 1, 2015, pp. 133-141.
- [9] L. Haiwei, D. Yuanhua, W. Haiyun and L. Yun, “Adsorption Behavior of Ammonium by a Bio Adsorbent – Boston Ivy Leaf Powder”, *Journal of Environmental Sciences*, Vol. 22, 2010, pp. 1513-1518.
- [10] M. Zhang, H. Zhang, D. Xu, L. Han, D. Niu, B. Tian, J. Zhang, L. Zhang and W. Wu, “Removal of Ammonium from Aqueous Solutions using Zeolithe Synthesized from Fly Ash by a Fusion Method”, *Desalination*, Vol. 271, 2011, pp. 111-121.
- [11] Y. Ranaporn and N. Duangkamol, “Rexcling Oyster Shell as Adsorbent for Phosphate Removal”, *Chemical Engineering and Applied chemistry*, Vol. 17, 2011, pp. 10-11.
- [12] P. Cai, H. Zheng, C. Wang, M. Hongwen, J. Hu, Y. Pu and P. Liang, “Competitive Adsorption Characteristics of Fluoride and Phosphate on Calcined Mg-Al- $\text{CO}_3$ ”, *Journal of Hazardous Materials*, Vol. 2012, 2014, pp. 100-108.
- [13] G. Dungan, Z. Xianzheng, V. Toulavanh, H. Minsheng, S. Li and H. Yan, “Phosphorus and Nitrogen Removal Using Novel Porous Brick Incorporated with Wastes and Minerals”, *Pollution Journal of Environmental Study*, Vol. 22, 2013, pp. 1349-1356.
- [14] C. Umpuch, “Batch adsorption of Organic Dyes by Organo-Bagasse: Carbon Content; pH Influence Kinetics and Isotherms”, *International Journal of Engineering*, Vol. 28, No. 4, 2015, pp. 507-515.
- [15] J. Ketcha Mbadcam, H. Ngomo Manga, J. Avom and D. D. Dina Joh, “Étude des Surface et Calcul Théorique des Sites Actifs de Charbons Actifs par Adsorption de l’Acide Tartrique”, *Déchets Sciences et Techniques*, Vol. 36, 2004, pp. 38-48.
- [16] R. Boopathy, S. Karthikeyan, A. B. Mandal and G. Sekaran, “Adsorption of Ammonium Ions by Coconut Shell-Activated Carbon from Aqueous Solution: Kinetic, Isotherm, and Thermodynamic Studies”, *Environmental Science and Pollution Research*, Vol. 19, No. 3, 2012, pp. 1-12.
- [17] D. Kučić, M. Markić and F. Briški, “Ammonium Adsorption on Natural Zeolite (Clinoptilolite: Adsorption Isotherms and Kinetics Modeling”, *The Holistic Approach to Environment*, Vol. 2, No. 4, 2012, pp. 145-158.
- [18] A. Demirak, F. Keskin, Y. Sahin and V. Kalenci, “Removal of Ammonium from Water by Pine Cone Powder as Biosorbent”, *Mugla Journal of Science and Technology*, Vol. 1, No. 1, 2015, pp. 5-12.
- [19] N. Jiwalak, S. Rattanaphani, J. B. Bremner and V. Rattanaphani, Equilibrium and Kinetic Modeling of the Adsorption of Indigo Carmine onto Silk, *Fibers and Polymers*, Vol. 11, No. 4, 2010, pp. 572-579.
- [20] H. Hegazi, “Removal of Heavy Metals from Wastewater using Agricultural and Natural Wastes as Adsorbents”, *Housing Building and Research Center*, Vol. 9, 2013, pp. 276-282.
- [21] B. A. Mohammed, “Removal of Textile Dyes (Maxilon Blue and Methyl Orange) by Date Stones Activated Carbon”, *International Journal of Advanced Research in Chemical Science*, Vol. 1, No. 1, 2014, pp. 45-59.
- [22] J. Ndi Nsami, J. Ketcha Mbadcam, S. Anagho Gabche, J. Ghogomu Numbonui and D. P. B. Belibi, “Physical and Chemical Characteristics of Activated Carbon Prepared by Pyrolysis of Chemically Treated Cola Nut (Cola Acuminata) Shells Wastes and Its Ability to Adsorb Organics”, *International Journal of Advanced Chemical Technology*, Vol. 3, No. 1, 2014, pp. 1-13.
- [23] J. Rhodier, B. Legube, N. Merlet et Col (9 édition), “Analyse de l’Eau”, Dunod, Paris, 2009, pp. 249-254.
- [24] D. Bendahou, T. D. Ainat and D. Bassou, “Adsorption du Cuivre Cu(II) en Solution par l’Argile Brute et Activée de la Région de Tiout-Naama Sud-Ouest Algérie”, *Revue Science des Matériaux*, Vol. 2, 2014, pp. 23-34.
- [25] M. Gourouza, A. Zanguina, Natatou and A. Boos, “Characterization of a Mixed Clay Niger”, *Sciences et Structure des Matériaux*, Vol. 1, 2013, pp. 1-11.
- [26] M. Wang, L. Liao, X. Zhang, Z. Li, Z. Xia and W. Cao, Adsorption of Low-Concentration Ammonium onto Vermiculite from Hebei Province, China, *Clays and Clays Minerals*, Vol. 59, No. 5, 2011, pp. 459-465.
- [27] Y. Subbareddy, C. Jayakumar, S. Valliammai, K. Nagaraja and B. Jeyaraj, “Equilibrium and Thermodynamic Study of Adsorption of Rhodamine B Dye from Aqueous Solution by Fuller’s Earth”, *International Journal of Research in Chemistry and Environment*, Vol. 4, No. 3, 2014, pp. 16-25.
- [28] A. M’leyeh, E. Srasra and A. Cheref, “Adsorption of Heavy Metals by Natural Clays of Borj Chekir, SW of Tunis”, *Proceedings of International Symposium on Environmental Pollution Control and Waste Management (EPCOWM’2002)*, (Tunis), January 7-10, 2002, pp. 533-546.
- [29] I. Tchakala, L. Bawa, G. Djaneye, K. Doni and P. Nambo, “Optimisation du Procédé de Préparation des Charbons Actifs par Voie Chimique ( $\text{H}_3\text{PO}_4$ ) à partir des Tourteaux de Karité et des Tourteaux de Coton”, *International Journal of Biological and Chemical Sciences*, Vol. 6, No. 1, 2012, pp. 461-478.
- [30] G. Fumba, J. S. Essomba, G. M. Tagne, J. Ndi Nsami, P. D. Belibi Belibi and J. Ketcha Mbadcam, “Equilibrium and Kinetic adsorption Studies of Methyl Orange from Aqueous Solutions Using Kaolinite, Metakaolinite and Activated Geopolymer as Low Cost Adsorbents”, *Journal of Academia and Industrial Research*, Vol. 3, No. 4, 2014, pp. 156-163.
- [31] K. Bennani, B. Mounir, M. Hachkar, M. Bakasse and A. Yaacoubi, “Élimination du Colorant Basique « Bleu de Méthylène » en Solution Aqueuse par L’argile de Safi”, *Revue des Sciences de l’Eau*, Vol. 23, No. 4, 2010, pp. 375-388.
- [32] J. S. Essomba, J. Ndi Nsami, P. D. Belibi Belibi, G. M. Tagne and J. Ketcha Mbadcam, “Adsorption of Cadmium (II) Ions from Aqueous Solution onto Kaolinite and Metakaolinite”, *Pure and Applied Chemical Sciences*, Vol. 2, No. 1, 2014, pp. 11-30.
- [33] J. Ndi Nsami and J. Ketcha Mbadcam, “The Adsorption Efficiency of Chemically Prepared Activated Carbon from Cola Nut Shells by  $\text{ZnCl}_2$  on Methylene Blue”, *Journal of Chemistry*, Vol. 2013, 2013, pp. 1-7.
- [34] A. Baybars, C. Özmetin and M. Korkmaz, “Cationic Dye (Methylene Blue) Removal from Aqueous Solution by Montmorillonite”, *Bulletin of Korean Chemistry Society*, Vol. 33, No. 10, 2012, pp. 1-7.
- [35] E. Ivanova, M. Karsheva and B. koumanova, “Adsorption of Ammonium Ions onto Natural zeolite”, *Journal of the University of Chemical Technology and Metallurgy*, Vol. 45, No. 3, 2010, pp. 295-303.
- [36] D. D. Dina Joh, N. Abdoul Rahman, J. Ndi Nsami and J. Ketcha Mbadcam, “Adsorption of Acetic Acid onto Activated Carbons Obtained from Maize Cobs by Chemical Activation with Zinc Chloride ( $\text{ZnCl}_2$ )”, *Research journal of Chemical Sciences*, Vol. 2, 2012, pp. 42-49.
- [37] J. Ketcha Mbadcam, H. Ngomo Manga, C. Tcheka, N. Abdoul Rahman, S. H. Djojo, and D. Kouotou, “Batch Equilibrium Adsorption of Cyanides from Aqueous Solution onto Copper and Nickel-Impregnated Powder Activated Carbon and Clay”, *Journal of Environmental Protection Science*, Vol. 3, 2009, pp. 53-57.
- [38] J. Ketcha Mbadcam, S. Dogmo and D. Dinka’a Ndaghu, “Kinetic and Thermodynamic Studies of the Adsorption of Nickel (II) Ions from Aqueous Solution by Smectite Clay from Sabga-Cameroon”, *International Journal of Current Research*, Vol. 4, No. 5, 2012, pp. 162-167.
- [39] A. H. Gedam, R. S. Dongre and A. K. Bansawal, “Synthesis and Characterization of Graphite Doped Chitosan Composite for Batch Adsorption of Lead (II) Ions from Aqueous Solution”, *Advanced Materials Letters*, Vol. 6, No. 1, 2015, pp. 59-67.
- [40] V. Venkasterwaran, P. Kalaamani and N. Karpagan, “Adsorptive Removal of Methylene Blue using Activated Prosopis Spicizera: A low-cost Adsorbent”, *Chemical Science Transaction*, Vol. 4, No. 2, 2015, pp. 347-354.
- [41] S. A. Bhalero, A. S. Sharma and S. D. Maind, “Removal of Zinc (II) Ions Using Peanut Hulls (Arachis hypogea linn) from Aqueous Solutions in a Batch System”, *International Journal of Advanced Research in Biology Sciences*, Vol. 2, No. 4, 2015, pp. 136-150.
- [42] K. Y. Foo and B. H. Hameed, Insights into the Modeling of Adsorption Isotherm System, *Chemical Engineering Journal*, Vol. 156, No. 2010, 2009, pp. 2-10.
- [43] B. A. Fil, M. T. Yilmaz, S. Bayar and M. T. Elkoca, Investigation of Adsorption of the Dye stuff Astrazon Red Violet 3RN (Basic Violet 16) on Montmorillonite Clay, *Brazilian Journal of Chemical Engineering*, Vol. 31, No. 1, 2014, pp. 171-182.

**Batch Adsorption of Ammonium Ions from Synthetic Wastewater using Local Cameroonian Clay and ZnCl<sub>2</sub> Activated Carbon**

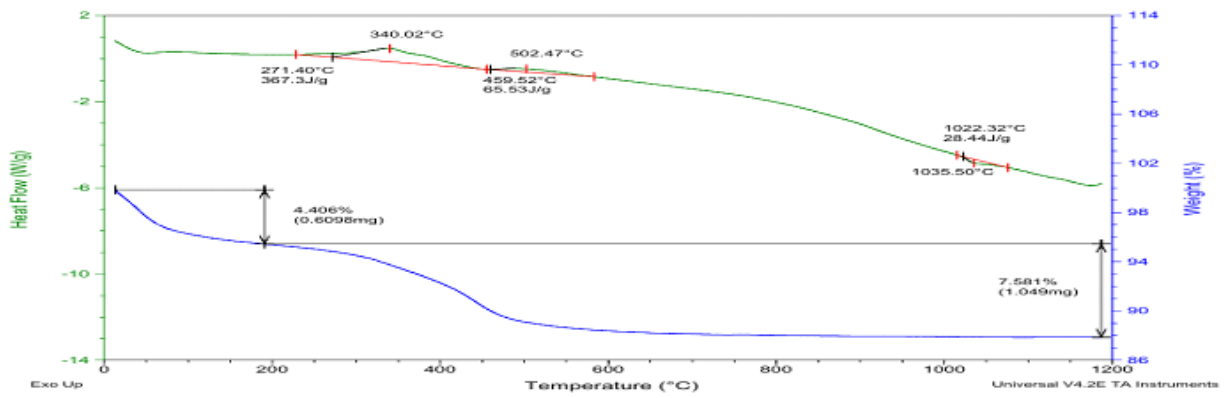


**Figure 1:** DSC (green line) – TGA (blue line) curves of the Soukamna Clay.

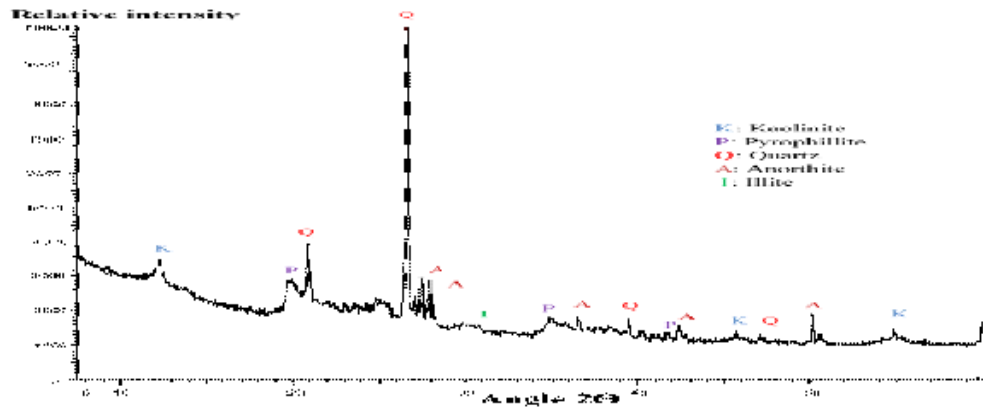


**Figure 2:** Diffractogram of Soukamna Clay.

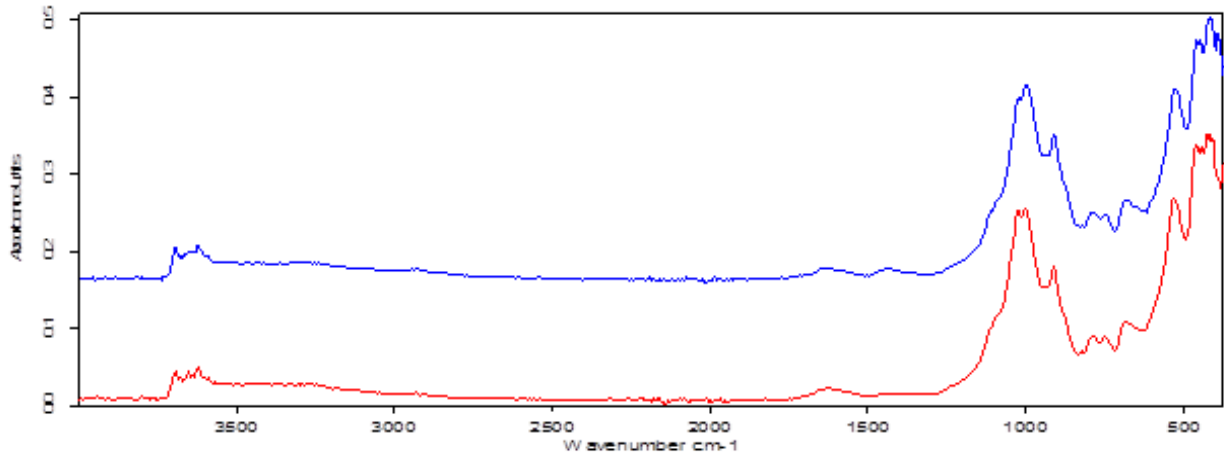


**Figure 3:** Superposition of infrared spectra of Soukamna Clay before (blue line) and after (red line) adsorption.

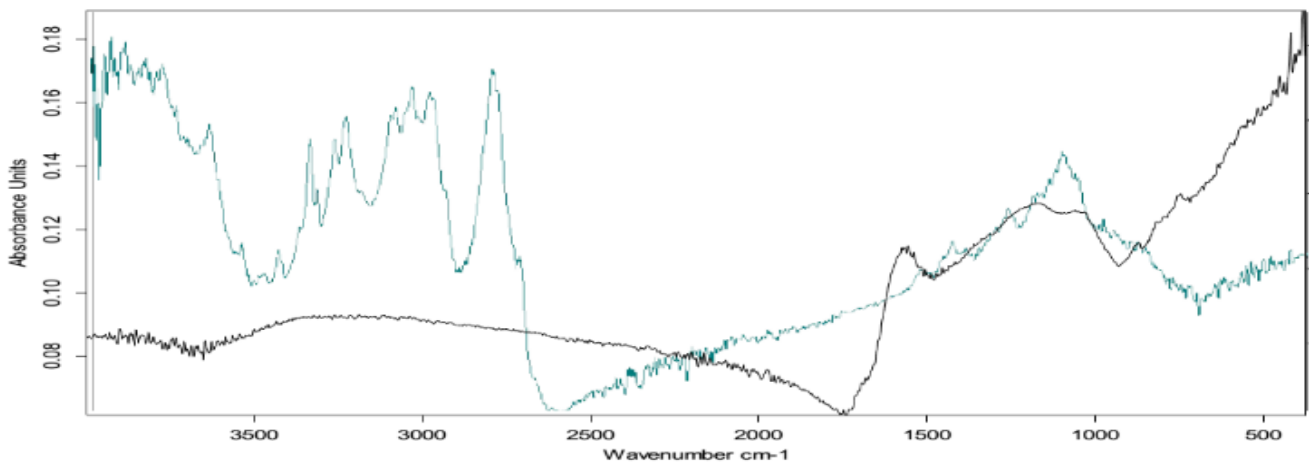


**Figure 4:** Superposition of infrared spectra of ZnCl<sub>2</sub> activated carbon before (black line) and after (green line) adsorption.

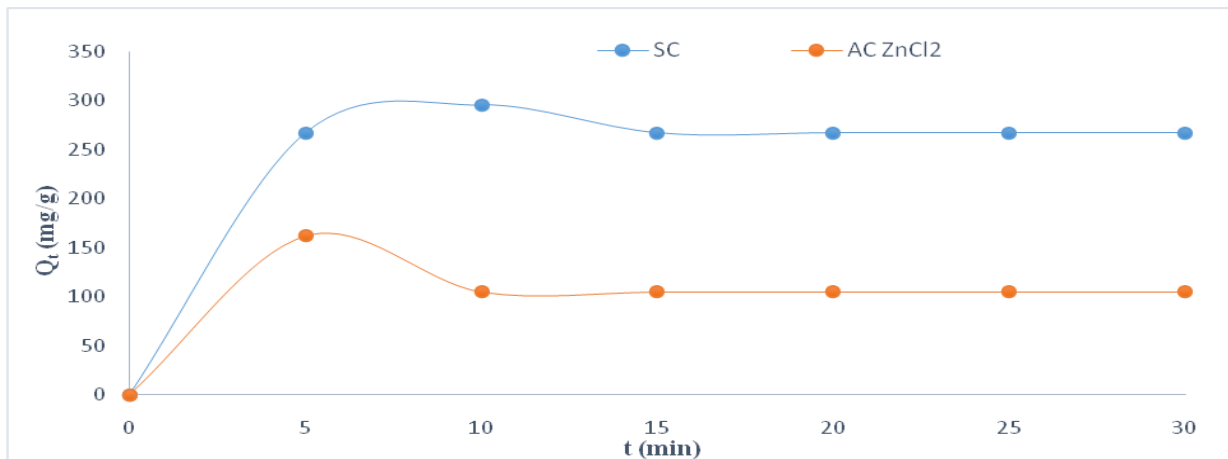


Figure 5: Effect of contact time on the adsorption of  $NH_4^+$  ions by SC and  $ZnCl_2$ -AC.

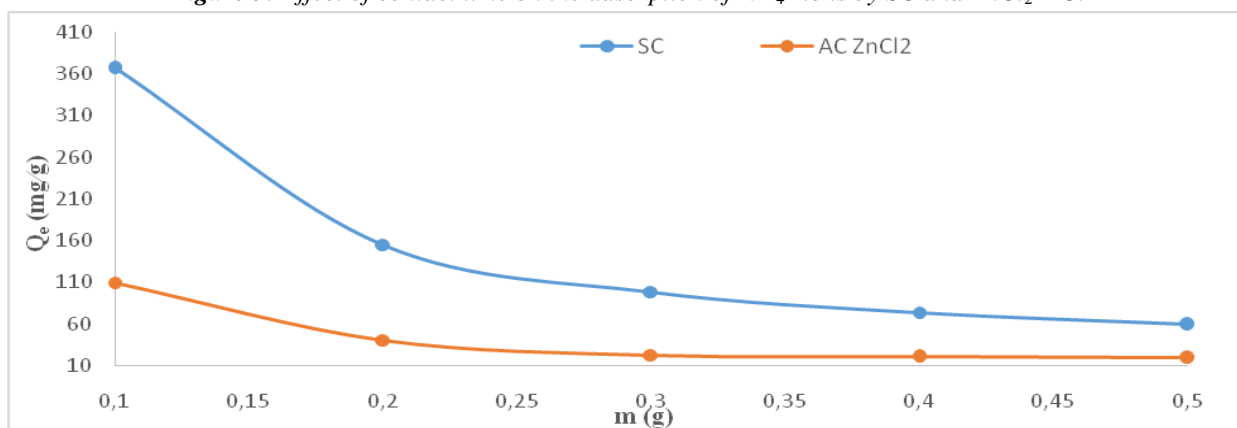


Figure 6: Effect of adsorbents dose on the adsorption of  $NH_4^+$  ions by SC and  $ZnCl_2$ -AC

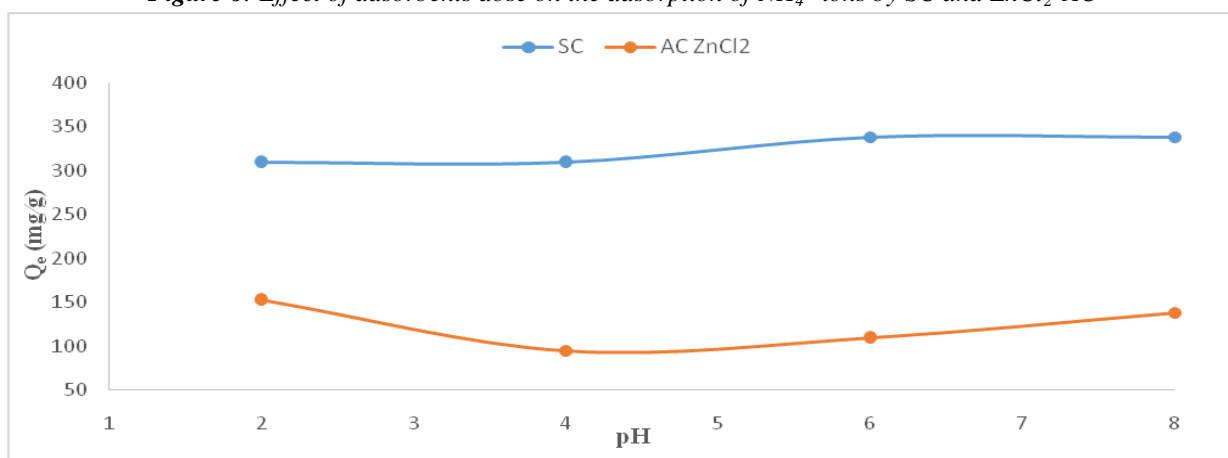


Figure 7: Effect of pH solution on the adsorption of  $NH_4^+$  ions by SC and AC  $ZnCl_2$ -AC.

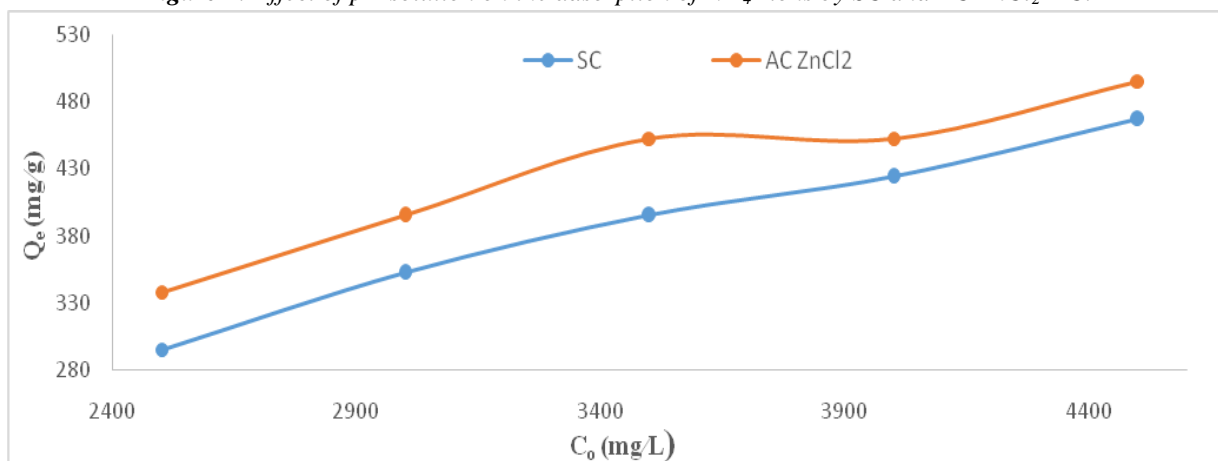
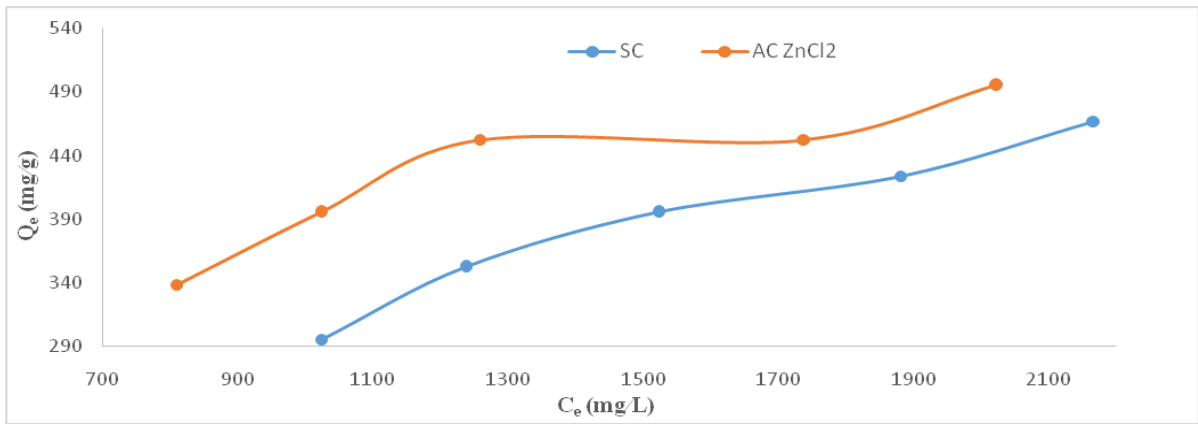
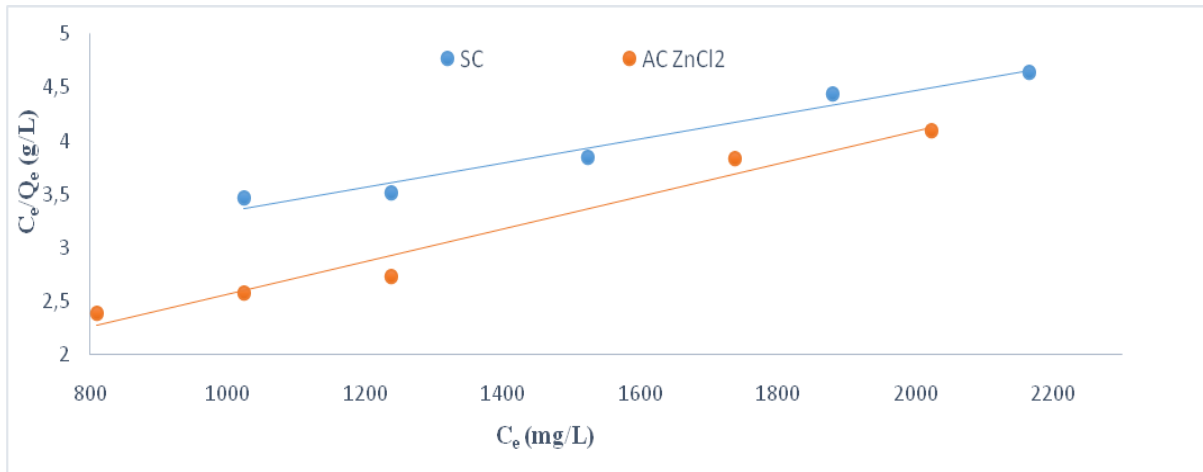


Figure 8: Effect of initial concentration on the adsorption of  $NH_4^+$  ions by SC and  $ZnCl_2$ -AC.

**Batch Adsorption of Ammonium Ions from Synthetic Wastewater using Local Cameroonian Clay and ZnCl<sub>2</sub> Activated Carbon**



**Figure 9:** Adsorption isotherms of NH<sub>4</sub><sup>+</sup> ions on SC and ZnCl<sub>2</sub>-AC.



**Figure 10:** Linear transform of Langmuir isotherm.

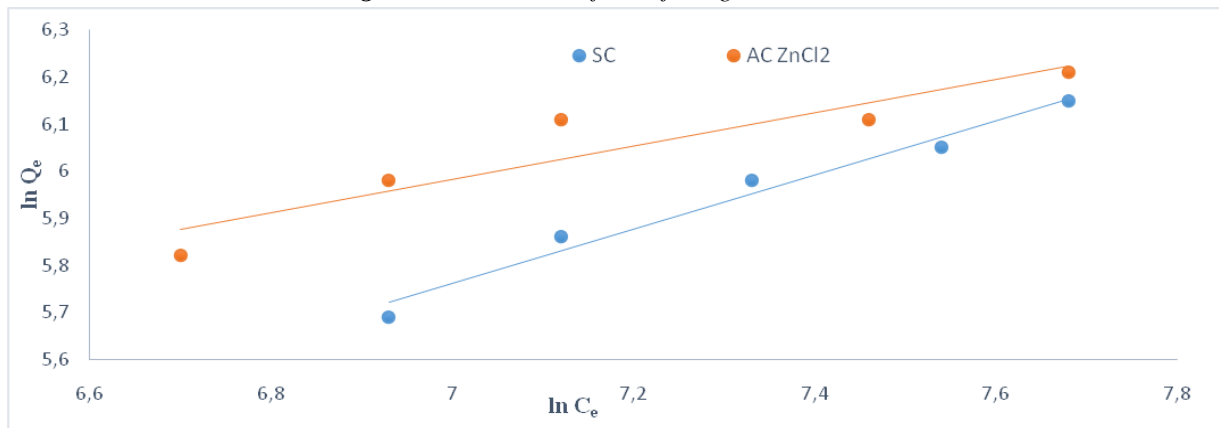


**Figure 11:** Linear transform of Freundlich isotherm.

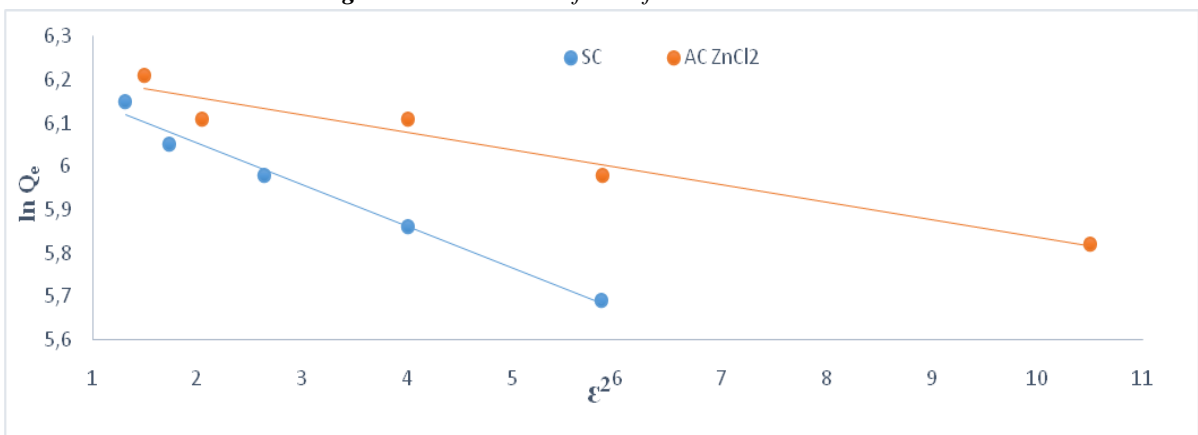


**Figure 12:** Linear transform of Dubinin-Kaganer-Raduskevich (D-K-R) isotherm.

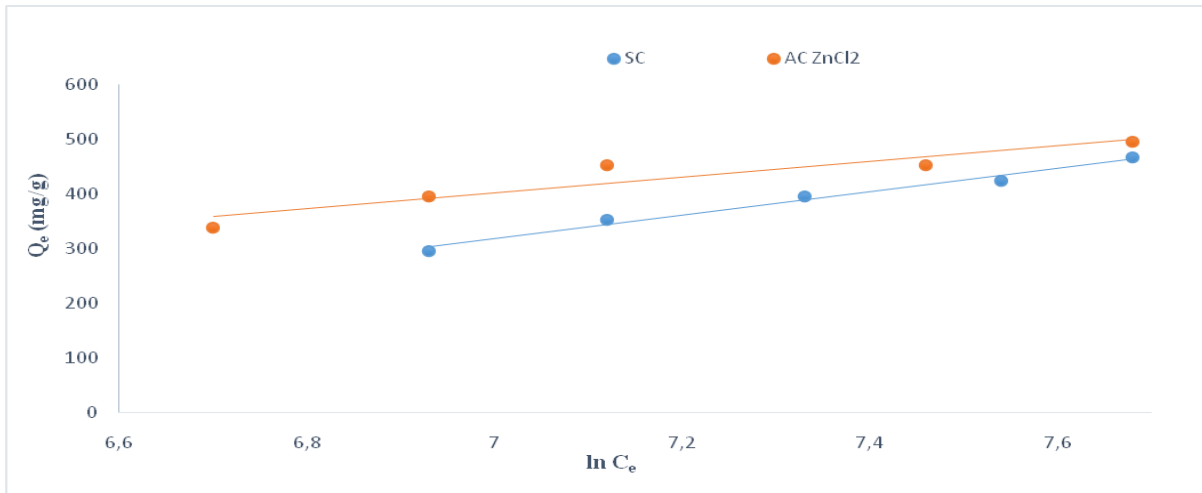


Figure 13: Linear transform of Temkin isotherm.



Figure 14: Pseudo-first order kinetic model.

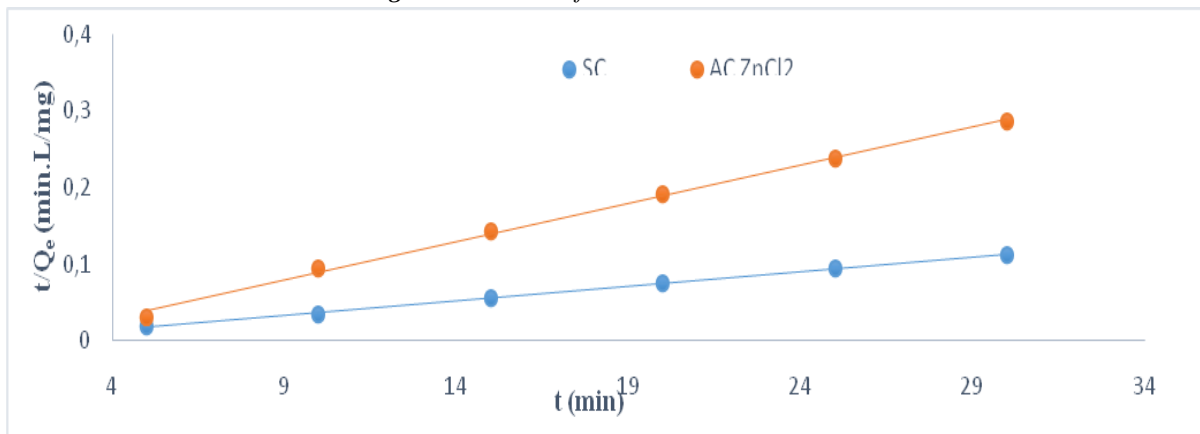
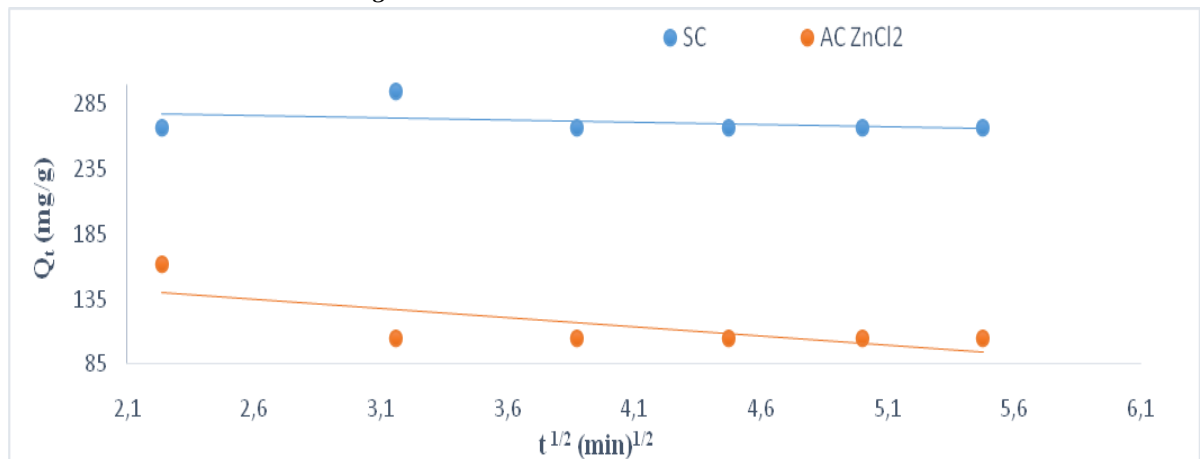
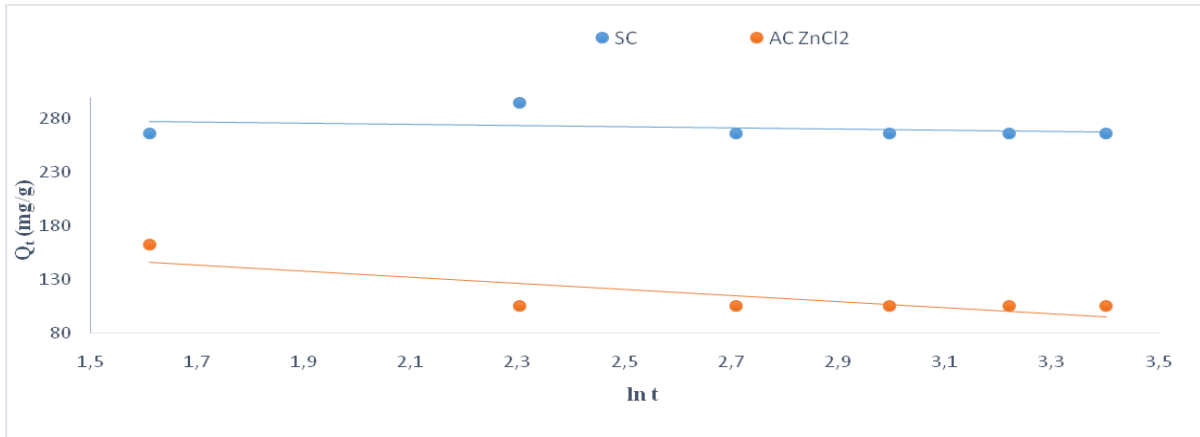


Figure 15: Pseudo-second order kinetic model.



**Batch Adsorption of Ammonium Ions from Synthetic Wastewater using Local Cameroonian Clay and ZnCl<sub>2</sub> Activated Carbon**

**Figure 16:** Intra-particle diffusion kinetic model.



**Figure 17:** Elovich kinetic model.

**Table 1:** Physico-chemical properties of Soukamna Clay and ZnCl<sub>2</sub> Activated Carbon.

Sample	Soukamna Clay	ZnCl <sub>2</sub> Activated Carbon
Specific surface area (m <sup>2</sup> /g)	42,2943	647,7374
Average pore width (nm)	10,13787	2,05059
Average pore diameter (nm)	11,1922	3,8013
Total volume of the pores (cm <sup>3</sup> /g)	0,107193	0,332061
Type of hysteresis	III	I

**Table 2:** Chemical composition of Soukamna Clay

Oxides	SiO <sub>2</sub>	Al <sub>2</sub> O <sub>3</sub>	Fe <sub>2</sub> O <sub>3</sub>	CaO	MgO	K <sub>2</sub> O	Na <sub>2</sub> O	SO <sub>3</sub>	TiO <sub>2</sub>	Mn <sub>2</sub> O <sub>3</sub>	P <sub>2</sub> O <sub>5</sub>	L.O.I**	Total
(%)*	61,49	18,00	7,40	1,69	0,56	3,10	0,76	0,05	1,42	0,09	0,07	5,40	100,03

\*Mass percentage, \*\* Loss on Ignition.

**Table 3:** Isotherms models [43].

Isotherms Models	Linear Forms	Plots	Slope	Ordinates at the origin
Langmuir	$\frac{C_e}{Q_s} = \frac{1}{Q_m K} + \frac{C_e}{Q_m}$ (3)	$\frac{C_e}{Q_s}$ versus $C_e$	$\frac{1}{Q_m}$	$\frac{1}{Q_m K}$
Freundlich	$\ln Q_e = \ln K_F + (1/n) \ln C_e$ (4)	$\ln Q_e$ versus $\ln C_e$	$\frac{1}{n}$	$\ln K_F$
D-K-R	$\ln Q_e = \ln Q_{max} - \frac{1}{2E_a} (RT \ln(1 + \frac{1}{C_e}))^2$ (5)	$\ln Q_e$ versus $(RT \ln(1 + \frac{1}{C_e}))^2$	$-\frac{1}{2E_a}$	$\ln Q_{max}$
Temkin	$Q_e = B \ln K_T + B \ln C_e$ (6)	$Q_e$ versus $\ln C_e$	B	$B \ln K_T$

K<sub>F</sub>: Freundlich isotherm constant (mg.g<sup>-1</sup>), K<sub>L</sub>: Langmuir isotherm constant (L.mg<sup>-1</sup>), 1/n: Adsorption intensity, Q<sub>e</sub>: Amount of ammonium ions per gram of the adsorbent at equilibrium (mg/g), Q<sub>max</sub>: Maximum monolayer coverage capacity (mg.g<sup>-1</sup>), C<sub>e</sub>: Equilibrium (residual) concentration of adsorbate in solution (mg.L<sup>-1</sup>), E<sub>a</sub>: Mean sorption energy of Dubinin–Kaganer–Radushkevich (kJ.mol<sup>-1</sup>), R: Universal gas constant (8.314 J.mol<sup>-1</sup>.K<sup>-1</sup>), T: Absolute temperature (K), K<sub>T</sub>: Temkin isotherm related to equilibrium binding constant (L.g<sup>-1</sup>), B<sub>T</sub>: Temkin isotherm constant.

**Tableau 4:** Correlation coefficients, experimental and calculated values of different isotherms.

Isotherms	Parameters	Adsorbents	
		SC	ZnCl <sub>2</sub> -AC
Langmuir	R <sup>2</sup>	<b>0.9687</b>	<b>0.9688</b>
	Q <sub>max,cal</sub> (mg/g)	909.0909	666.6667
	Q <sub>max,exp</sub> (mg/g)	466.7143	495.2857
	K <sub>L</sub> x 10 <sup>4</sup> (L/mg)	4.985	14.200
Freundlich	R <sup>2</sup>	<b>0.9705</b>	<b>0.8681</b>
	K <sub>F</sub> (mg <sup>1-1/n</sup> .L <sup>1/n</sup> /g)	5.5575	30.00
	$\frac{1}{n}$	0.5729	0.3694
D-K-R	R <sup>2</sup>	<b>0.9865</b>	<b>0.9494</b>
	Q <sub>m,cal</sub> (mmol/g)	28.4877	28.8836
	Q <sub>m,exp</sub> (mmol/g)	27.4518	27.8682
	E (J/mol)	2.2954	3.3186
Temkin	R <sup>2</sup>	<b>0.9836</b>	<b>0.8786</b>
	b <sub>T</sub> (J/mol)	11.5257	17.1411
	K <sub>T</sub> x 10 <sup>3</sup> (L/g)	4.0017	14.6174

**Table 5:** Kinetic Models[44].

Kinetic Models	Linear Forms	Plots	Slope	Ordinates at the origin
Pseudo-first order	$\ln(Q_e - Q_t) = \ln Q_e - K_1 t$ (7)	Ln (Q <sub>e</sub> -Q <sub>t</sub> ) versus t	K <sub>1</sub>	lnQ <sub>e</sub>
Pseudo-second order	$\frac{t}{Q_t} = \frac{1}{K_2 Q_e^2} + \frac{t}{Q_e}$ (8)	$\frac{t}{Q_t}$ versus t	$\frac{1}{Q_e}$	$\frac{1}{K_2 Q_e^2}$
Intraparticle diffusion	Q <sub>t</sub> = K <sub>id</sub> t <sup>1/2</sup> + C <sub>i</sub> (9)	Q <sub>t</sub> versus t <sup>1/2</sup>	K <sub>id</sub>	C <sub>i</sub>
Elovich	Q <sub>t</sub> = $\frac{1}{\beta} \ln(\alpha\beta) + \frac{1}{\beta} \ln t$ (10)	Q <sub>t</sub> versus ln t	$\frac{1}{\beta}$	$\frac{1}{\beta} \ln(\alpha\beta)$